

Competitive Brownian and Lévy walkers

E. Heinsalu,^{1,2} E. Hernández-García,¹ and C. López¹

¹*IFISC, Instituto de Física Interdisciplinar y Sistemas Complejos (CSIC-UIB),
Campus Universitat de les Illes Balears, E-07122 Palma de Mallorca, Spain*

²*National Institute of Chemical Physics and Biophysics, Rāvala 10, Tallinn 15042, Estonia*
(Dated: November 18, 2011)

Population dynamics of individuals undergoing birth and death and diffusing by short or long ranged twodimensional spatial excursions (Gaussian jumps or Lévy flights) is studied. Competitive interactions are considered in a global case, in which birth and death rates are influenced by all individuals in the system, and in a nonlocal but finite-range case in which interaction affects individuals in a neighborhood (we also address the noninteracting case). In the global case one single or few-cluster configurations are achieved with the spatial distribution of the bugs tied to the type of diffusion. In the Lévy case long tails appear for some properties characterizing the shape and dynamics of clusters. Under non-local finite-range interactions periodic patterns appear with periodicity set by the interaction range. This length acts as a cut-off limiting the influence of the long Lévy jumps, so that spatial configurations under the two types of diffusion become more similar. By dividing initially everyone into different families and following their descent it is possible to show that mixing of families and their competition is greatly influenced by the spatial dynamics.

PACS numbers: 05.40.-a, 05.40.Fb, 87.18.Hf, 87.23.Cc

I. INTRODUCTION

Birth and death are the most relevant processes in determining the dynamics of biological populations which in the context of statistical physics can be modeled using interacting particle models where particle number is changing in time. As it is understood by now, birth and death processes are also responsible for clustering mechanisms in systems where random-walking individuals undergo reproduction and death. As a result, aggregation of organisms can occur even in simple models where birth and death processes are combined with spatial diffusion. In fact, in the most simple *Brownian bug model*, where particles reproduce and die with the same probability and undergo Brownian motion [1–3], clustering of particles was observed. In this model the clustering is produced simply by the reproductive correlations (the offspring is born at the same location of the parent) and by the irreversibility of the death process. Birth and death models of moving individuals are the pertinent framework to capture properties of biological systems such as planktonic populations [2], or patterns in amoebae [4] and bacteria [5].

Taking into account another central ingredient that is present in ecological systems, namely, the competition with other individuals in the neighborhood for resources, the formation of periodic spatial structures was observed in Refs. [6–8]. In these *nonlocally interacting Brownian bug models* it was assumed that the reproduction probability depends on the number of other organisms in the neighborhood. In Ref. [9] *nonlocally interacting Lévy bugs*, i.e., reproducing and dying organisms that undergo Lévy flights, were studied. This type of motion is relevant to model cell migration [10], biological searching strategies [11, 12], bacteria dynamics [13], or pattern formation of mussels [14]. In Ref. [9] it was shown that the forma-

tion of a periodic pattern is robust with respect to the type of spatial motion that the particles perform. The periodic arrangement of clusters in these nonlocally interacting bug models is a consequence of the competitive interaction and has a spatial scale determined by the interaction range [6]. However, a deeper analysis of the differences and similarities between the Brownian and Lévy cases is still missing. In particular, as shown in [7, 15], this analysis can be very conveniently performed by considering the limit of the interaction distance reaching the system size (global interaction), since a unique cluster appears which helps to understand and characterize the cluster properties, and the fluctuations of the population size.

In the present paper we report on differences between the systems of Brownian and Lévy bugs, in the situations of global and non-local interactions, as well as in the non-interacting case. In addition, results on the dependence of population on diffusion, and mixing of *families* of particles are presented for the finite-range interaction case. The paper is organized as follows: in Sec. II we describe the models to be analyzed. In Sec. III the noninteracting bug systems are studied. The infinite competition range where each particle is competing with all the others is analyzed in Sec. IV. Finally, the nonlocally interacting (i.e. with a finite interaction range) models are investigated in Sec. V.

II. MODEL AND NUMERICAL ALGORITHM

We consider a system consisting initially of N_0 point-like particles, which could be thought as being biological organisms or bugs, placed randomly in a two-dimensional $L \times L$ square domain with periodic boundary conditions. Except when explicitly stated, we take $L = 1$,

so that lengths are measured in units of system size. Bugs diffuse, reproduce at rate r_b^i , and die at rate r_d^i ; $i = 1, \dots, N$, and $N \equiv N(t)$ is the number of bugs in the system at time t . The numerical algorithm used to evolve the system follows the one suggested in Ref. [16]. The following sequence of steps is repeated until the final simulation time is reached:

We first compute the random time τ after which the next demographic event (birth or death) will occur. For this we need to determine the total birth and death rates,

$$B_{\text{tot}} = \sum_{i=1}^N r_b^i, \quad D_{\text{tot}} = \sum_{i=1}^N r_d^i, \quad (1)$$

and compute also the total rate

$$R_{\text{tot}} = B_{\text{tot}} + D_{\text{tot}} = \sum_{i=1}^N (r_b^i + r_d^i). \quad (2)$$

For the random times τ we choose an exponential probability density with the complementary cumulative distribution

$$p(\tau) = \exp(-\tau/\tilde{\tau}) \quad (3)$$

so that values of τ could be generated from $\tau = -\tilde{\tau} \ln(\xi_0)$, where ξ_0 is a uniform random number on $(0, 1)$ [17]. The characteristic time or time-scale parameter $\tilde{\tau} = \langle \tau \rangle$ is determined by the total rate:

$$\tilde{\tau} = R_{\text{tot}}^{-1}. \quad (4)$$

After the random time τ , an individual i , chosen among all the $N(t)$ bugs, either reproduces or disappears. With probability $B_{\text{tot}}/R_{\text{tot}}$ the event is reproduction and with probability $D_{\text{tot}}/R_{\text{tot}}$ it is death. The probability of choosing a particular individual i is weighted proportionally to its contribution to the corresponding total rate. In the case of reproduction, the new bug is located at the same position (x_i, y_i) as the parent individual i . Finally, all the bugs perform a jump of random length ℓ in a random direction characterized by an angle uniformly distributed on $(0, 2\pi)$ (ℓ and the direction of the jump are independent for each particle). The new present time is $t + \tau$, bugs are relabeled with indices $i = 1, 2, \dots, N(t + \tau)$, and the process is repeated.

When bugs undergo normal diffusion (Brownian bugs), a Gaussian jump-length probability density function is used,

$$\varphi(\ell) = \frac{2}{\tilde{\ell}\sqrt{2\pi}} \exp\left(-\frac{\ell^2}{2\tilde{\ell}^2}\right), \quad \ell \geq 0 \quad (5)$$

with second moment $\langle \ell^2 \rangle = \tilde{\ell}^2$; $\tilde{\ell}$ is the space-scale parameter. Since we draw the angle specifying the direction of the jump from the interval $(0, 2\pi)$, we restrict ℓ in Eq. (5) to have positive sign. The random jump length ℓ can be computed from $\ell = \tilde{\ell} \xi_G$, where ξ_G is sampled from the

standard Gaussian distribution with average 0 and standard deviation 1, and neglecting the sign. Note that the random walk defined in this way is not exactly the same as the one in which the walker performs jumps extracted from a two-dimensional Gaussian distribution, but it also leads to normal diffusion and allows a more direct comparison with the Lévy case. The corresponding diffusion coefficient can be estimated as

$$\kappa = \langle \ell^2 \rangle / (2\langle \tau \rangle) = \tilde{\ell}^2 / (2\tilde{\tau}). \quad (6)$$

As we choose to fix the value of κ , and the demographic rates, then the space-scale parameter is determined by

$$\tilde{\ell} = \sqrt{2\kappa\tilde{\tau}} = \sqrt{2\kappa/R_{\text{tot}}}. \quad (7)$$

In order to simulate the system where the bugs undergo superdiffusive Lévy flights (Lévy bugs) one can use a symmetric Lévy-type probability density function for the jump size ($\ell \geq 0$), behaving asymptotically as [18, 19]

$$\varphi_\mu(\ell) \approx \tilde{\ell}^\mu |\ell|^{-\mu-1}, \quad \ell \rightarrow \infty \quad (\ell \gg \tilde{\ell}) \quad (8)$$

with the Lévy index $0 < \mu < 2$. For all Lévy-type probability density functions with $\mu < 2$ the second moment diverges, $\langle \ell^2 \rangle = \infty$, leading to the occurrence of extremely long jumps, and typical trajectories are self-similar, showing at all scales clusters of shorter jumps interspersed with long excursions. For $0 < a < \mu < 2$ fractional moments $\langle \ell^a \rangle$ are finite. For the Lévy index in the range $1 < \mu < 2$ the value of $\langle \ell \rangle$ is finite. The complementary cumulative distribution corresponding to (8) behaves as

$$P_\mu(\ell) \approx \mu^{-1} (\ell/\tilde{\ell})^{-\mu}, \quad \ell \rightarrow \infty. \quad (9)$$

As a simple form of complementary cumulative distribution function which behaves asymptotically as (9), we use

$$P_\mu(\ell) = (1 + b^{1/\mu} \ell/\tilde{\ell})^{-\mu}, \quad (10)$$

with $b = [\Gamma(1 - \mu/2)\Gamma(\mu/2)]/\Gamma(\mu)$, and $\ell \geq 0$. As before, the direction of the jump is assigned by drawing a random angle on $(0, 2\pi)$. The particular expression for b is chosen for consistency with previous work [9]. It gives to the tail of the jump distribution the same prefactor as for the Lévy-stable distribution [20], but any other positive value of b should lead to the same results reported here. One can generate a random step-length ℓ by inverting (10):

$$\ell = \tilde{\ell} \frac{(\xi_0^{-1/\mu} - 1)}{b^{1/\mu}}. \quad (11)$$

with ξ_0 being a uniform random variable on the unit interval. Now the diffusion coefficient (6) is infinite, but one can define a generalized diffusion coefficient in terms of the scales $\tilde{\ell}$ and $\tilde{\tau}$ as [18, 19]

$$\kappa_\mu = \tilde{\ell}^\mu / (2\tilde{\tau}). \quad (12)$$

Therefore, in the case of the Lévy flights, when fixing the value of κ_μ , the space-scale parameter is:

$$\tilde{\ell} = (2\kappa_\mu \tilde{\tau})^{1/\mu} = (2\kappa_\mu / R_{\text{tot}})^{1/\mu}. \quad (13)$$

As we consider the bugs to be point-like, the spatial dynamics does not include any interaction between them. The interaction is instead taken into account through reproduction and death rates, which we assume to be affected by competitive interactions.

If the birth and death rates of a bug are influenced by the number of other bugs within a certain radius R , one talks about a *nonlocal interaction* of finite range. In the present paper we assume that the birth and death rates of the i -th individual depend linearly on the number of neighbors in the interaction range [6],

$$r_b^i = \max(0, r_{b0} - \alpha N_R^i), \quad (14)$$

$$r_d^i = \max(0, r_{d0} + \beta N_R^i). \quad (15)$$

Here N_R^i is the number of bugs which are at a distance smaller than R from bug i , the parameters r_{b0} and r_{d0} are the zero-neighbor birth and death rates, and the parameters α and β determine how r_b^i and r_d^i depend on the neighborhood. For positive values of α and β , the more neighbors an individual has within the radius R , the smaller is the probability for reproduction and the larger is the probability that the bug does not survive, which could arise from competition for resources. The function $\max()$ enforces the positivity of the rates. Since we take $R < L/2$ (in fact $R \ll L$), the periodic boundary conditions are straightforwardly implemented and bugs are never counted twice.

If the birth and death rates of a bug are instead influenced by all the other individuals in the system, i.e.,

$$r_b^i \equiv r_b = \max\{0, r_{b0} - \alpha[N(t) - 1]\}, \quad (16)$$

$$r_d^i \equiv r_d = \max\{0, r_{d0} + \beta[N(t) - 1]\}, \quad (17)$$

then one talks about *global interaction*. This is formally equivalent to Eqs. (14) and (15) with R sufficiently large for the interaction domain to include the whole system, but taking care of counting each bug only once, so that $N_R^i = N(t) - 1$.

In the case the rates of the demographic events are the same for all the bugs and assume constant values,

$$r_b^i \equiv r_b = r_{b0}, \quad r_d^i \equiv r_d = r_{d0}, \quad (18)$$

which is equivalent to $\alpha = \beta = 0$ in Eqs. (14), (15), bugs are *noninteracting*.

In the following we discuss the Brownian and Lévy bug systems when individuals do not influence each other and when inter-particle interaction occurs, either global or nonlocal. Although we formally maintain the parameter β in Eqs. (15) and (17), in our numerical examples we restrict to $\beta = 0$.

III. SIMPLE BUG MODELS WITH NO INTERACTION

A. Noninteracting Brownian bugs

The simple Brownian bug model with no interaction, i.e., when the birth and death rates of the individuals are given by Eq. (18), has been studied and discussed in various works [1, 2]. The ensemble average of the total population size follows

$$\langle N(t) \rangle = N_0 \exp[\Delta(t - t_0)], \quad (19)$$

independently of the diffusivity of the bugs; it only depends on the difference $\Delta = r_b - r_d$. If the birth rate is larger than the death rate, $\Delta > 0$, the total population generally explodes exponentially, though there is a finite probability for extinction that depends on the initial size of the population and decreases with increasing Δ . If the death rate is larger than the birth rate, $\Delta < 0$ the extinction of the population takes place with probability 1. If birth and death are equally probable, $\Delta = 0$, then the average over many realizations is $\langle N(t) \rangle = N_0$ and the average lifetime is infinite. However, in single realizations the fluctuations in the number of individuals are huge leading to fast extinction in some runs. In fact, there exists a typical lifetime proportional to N_0 , defined as the time for which the fluctuations become as large as the mean value, beyond which the population is extinct with probability close to 1 [1].

As a surprising effect, in the systems where the noninteracting Brownian bugs undergo death and reproduction with equal probabilities, spatial clustering of the bugs was observed in single realizations [1–3]. A typical time evolution of such a system is illustrated in Fig. 1a. We note that in all figures presenting the spatial configurations of the bugs, we have divided the individuals according to their initial position into nine groups characterized by different colors as in Fig. 1 at time $t = 0$; if reproduction takes place, the newborn bug assumes the same color as the parent. From Fig. 1a one can see that many small clusters form some time after starting from a uniform initial distribution. The occurrence of the clustering is related to the fact that in the case of reproduction the new bug is located at the same position as the parent. Due to the fluctuations and irreversibility of death the number of clusters decreases in time, until there will be a single cluster consisting of individuals coming from a single ancestor. There are constant, spontaneous, short-lived break-offs from the main cluster, which are always located near it. The center of mass of such a cluster undergoes a motion similar to that of a single bug [1] and its linear width fluctuates with a typical value proportional to $\sqrt{N_0}$ [1]. Furthermore, the larger the diffusion coefficient κ , the wider is the cluster (notice that when simulating the system numerically, if the diffusivity becomes so large that the jump lengths become comparable to the system size, one needs to take a larger simulation

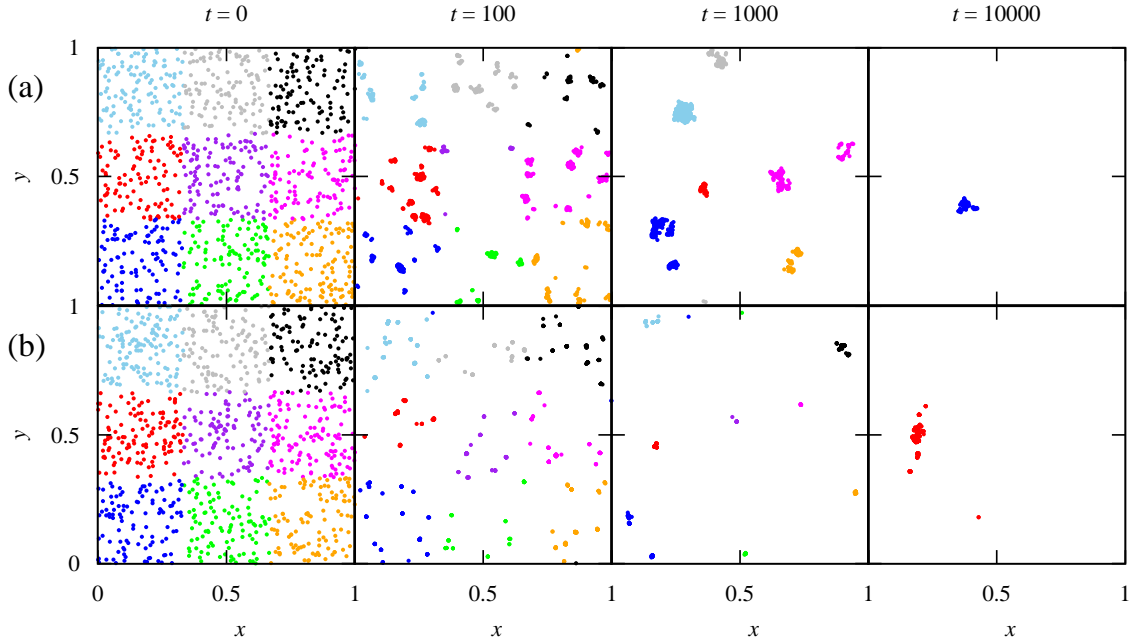


FIG. 1: (Color) Simple bug models with no interaction; spatial configuration of bugs at different times t : (a) Brownian bugs with $\kappa = 10^{-6}$ and (b) Lévy bugs with $\kappa_\mu = 10^{-5}$ and $\mu = 1$. Reproduction and death occur with equal probability, $r_b = r_d = 0.1$, and the initial number of individuals is $N_0 = 1000$. Bugs are colored with the color their ancestors bear in the panel at $t = 0$.

box). Finally, due to the fluctuations also the last cluster disappears.

B. Noninteracting Lévy bugs

In the case of noninteracting Lévy bugs, the number of individuals still follows Eq. (19), independently of the Lévy index μ , and also the cluster formation observed in the case of Brownian bugs takes place. Now, however, as bugs can perform long jumps, there are also small clusters continuously appearing and disappearing far from the main clusters (Fig. 1b). The smaller the value of μ the more anomalous the system, i.e., the larger is the probability for long jumps and therefore there are more flash-clusters. When the number of clusters has already decreased to one, due to the long jumps and fluctuation of the number of individuals, new clusters that are placed far from the central cluster can appear in the system also for some time and often the disappearance of the main cluster takes place whereas another new central cluster appears somewhere else. As a result the center of mass undergoes anomalous diffusion as single bugs do. The value of the Lévy index μ influences also the linear size of the main clusters: the smaller is μ , the more compact are the clusters, although also more particle jumps to long distances occur. The influence of the value of κ_μ is similar as in the case of Brownian bugs, i.e., a larger value of the anomalous diffusion coefficient results in a larger linear size of the clusters.

IV. GLOBAL INTERACTION

A. Formation of a cluster

Let us now investigate the behavior of the Brownian and Lévy bug systems in the case of global interaction, i.e., birth and death rates of the individuals are given by Eqs. (16), (17). The time evolutions of the globally interacting Brownian and Lévy bug systems are illustrated by Fig. 2a and 2b, respectively. In both systems we start from $N_0 = 500$ bugs uniformly distributed in the simulation area and choose for the parameters characterizing death and birth rates the following values: $r_{b0} = 1$, $r_{d0} = 0.1$, $\alpha = 0.02$, $\beta = 0$. As in the noninteracting case, the final state of the dynamics is complete extinction, since there is always a nonvanishing probability for a fluctuation strong enough to produce that. However, if the number of bugs in the system is large this happens at very long times [21]. Then, there is a long-lived *quasi-stable* state for which the average number of individuals $\langle N(t) \rangle$ can be estimated from the condition that death and birth are equally probable, $r_b^i = r_d^i$. From there,

$$\langle N(t) \rangle = \frac{\Delta_0}{\alpha + \beta} + 1, \quad (20)$$

where $\Delta_0 = r_{b0} - r_{d0}$. We have restricted to parameter values so that the max functions in Eqs. (16-17) do not operate. Since we have chosen $N_0 > \langle N(t) \rangle = 46$ in Fig. 2, death is more probable at small times and the number of bugs decreases rapidly. Approximately at time $t = 30$ the number of individuals has reached the value at which

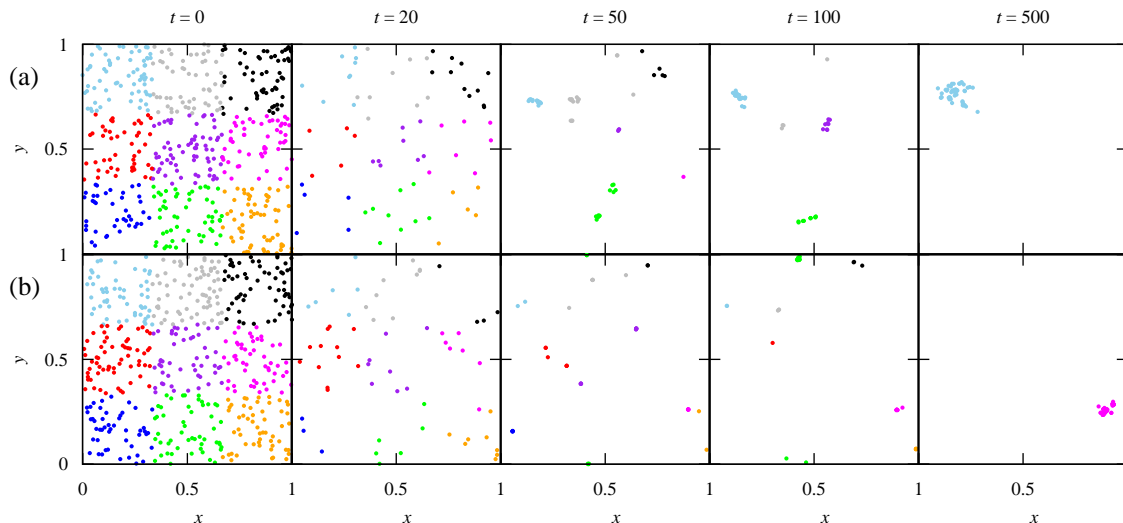


FIG. 2: (Color) Globally interacting bug models; spatial configuration of bugs at different times t : (a) Brownian bugs with $\kappa = 10^{-5}$ and (b) Lévy bugs with $\kappa_\mu = 10^{-4}$ and $\mu = 1$. The parameters in the reproduction and death rates are: $r_{b0} = 1$, $r_{d0} = 0.1$, $\alpha = 0.02$, $\beta = 0$. Bugs are colored with the color their ancestors bear in the panel at $t = 0$.

death and birth become in average equally probable and after this time particle number fluctuates around that value; parameters of the birth and the death rates can be chosen so that these fluctuations are weak. At this time small clusters start to form due to the reproductive pair correlations. As in the case of noninteracting bugs, fluctuations and irreversibility of death makes the number of clusters to decrease in time, although now the fluctuations of the particle content of the different clusters are correlated to keep the total number close to the value given by Eq. (20) and the process is faster. Finally a single cluster consisting of bugs coming from the same ancestor remains (as stated before, it will also disappear at very long times due to finite-size fluctuation effects) though there are also now spontaneous short-lived break-offs from the central cluster as in the case of noninteracting bugs. The center of mass of such a cluster is moving in space and its linear size is a fluctuating quantity. The clustering of the globally interacting bugs was quantitatively discussed in Ref. [7] for the one-dimensional Brownian bug system.

B. Fluctuations of the number of bugs

As indicated by Eq. (20), for given values of α and β , the average number of individuals in the system with global interaction depends solely on the difference $\Delta_0 = r_{b0} - r_{d0}$. It is independent of the concrete values of r_{b0} and r_{d0} , as well as of the value of κ or κ_μ and μ ; in fact, it does not even depend on whether the system consists of Brownian or Lévy bugs. Nevertheless, fluctuations of the number of bugs do indeed depend on the values of r_{b0} and r_{d0} , even if the difference Δ_0 , and thus the average number of bugs, has the same value. To illustrate this, let us

calculate from the simulations time series the probability distribution of the number of individuals in the globally interacting Brownian and Lévy bug systems. As can be seen from Fig. 3, for a given value of Δ_0 , larger values of r_{b0} and r_{d0} lead to larger fluctuations. This is a simple consequence of the Poisson character of the birth and death events for which fluctuations in each of the instantaneous rates are proportional to the mean rates. When the distributions are narrow, they are close to Gaussian. For larger rates particle number distribution gets broader implying that there is an enhanced probability that particle number becomes zero at some moment, after which bugs become extinct (remember that what is in fact plot in Fig. 3 is the numerical particle number distribution in the long-lived metastable state before extinction). For the present case with $\Delta_0 = 0.9$ and $\alpha = 0.02$, $\beta = 0$, rate values above the ones shown in Fig. 3 (i.e. $r_{b0} > 2$, $r_{d0} > 1.1$) lead to observable extinction after some tenths of thousands of steps. An ecological implication of this could be the following: one can think of two colonies of organisms of the same type, having both the same equilibrium size determined for example by the size of the living area. Now if in one of the systems the population has no enemies and the natural death rate is low, but in the other the death rate is higher due to the presence of a predator, then the latter system will more probably go to extinction sooner due to the presence of larger fluctuations.

C. The average cluster shape, cluster width, and center of mass motion

Let us keep in the following $\alpha = 0.02$, $\beta = 0$ and $r_{b0} = 1$, $r_{d0} = 0.1$ [the same parameter values as in

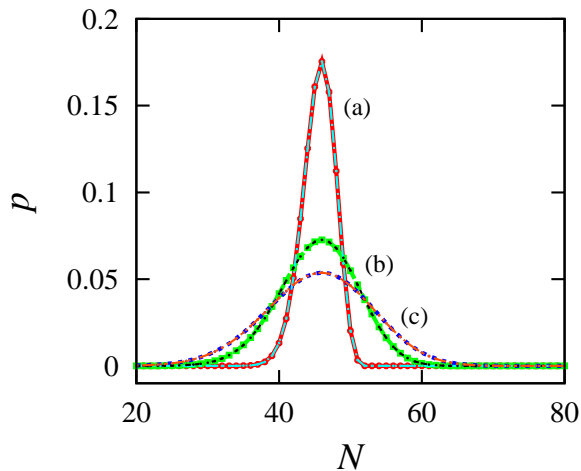


FIG. 3: (Color online) Probability distribution of the number of bugs in globally interacting bug systems. The results are numerically obtained from the time series of the particle number in the very long-lived state before the fluctuations lead the system to the extinction. For all the curves $\alpha = 0.02$, $\beta = 0$, and the rate difference is $\Delta_0 = r_{b0} - r_{d0} = 0.9$, but the rates r_{b0} , r_{d0} assume different values: (a) $r_{b0} = 1$, $r_{d0} = 0.1$; (b) $r_{b0} = 1.5$, $r_{d0} = 0.6$; (c) $r_{b0} = 2$, $r_{d0} = 1.1$. The overlapping curves correspond to Brownian and Lévy bug systems; the distributions do not depend on the type of diffusion nor on the values of κ , κ_μ or μ in this globally interacting case.

Fig. 2 and in Fig. 3 for curve (a)] and study the behavior of the cluster formed in the case of a system with global interaction defined by Eqs. (16)-(17). As mentioned, even after the transition from an uniform distribution of bugs to a single cluster (and before eventual extinction at large times), at some moment the system can consist actually of more than one cluster. In such cases we define that all the individuals in the system belong to the same cluster, even though in the Lévy case the distance between the bugs (subclusters) can be rather large. In order to avoid the boundary effects as much as possible, in Figs. 4-7 the linear size of the simulation area was taken as $L = 1000$ and to have enough statistics simulations were run until $t = 5 \times 10^8$.

Let us start by analyzing the average shape of the cluster. The average cluster, $\rho(x, y)$, is obtained setting at each time the origin in the center of mass of the cluster (distances under the periodic boundary conditions are computed under a minimum distance convention) and averaging over a long time (after the transition from uniform distribution to one single cluster but before long-time extinction). A one-dimensional cut of it (say across x for $y = 0$, i.e., $\rho(x) \equiv \rho(x, y = 0)$) is shown in Figs. 4 and 5. For the case of Brownian bugs, the tail of the average cluster is approximately exponential. A pair distribution function, which should be related but not identical to the average cluster discussed here, was analytically calculated in Ref. [16] for a globally interacting Brownian bug model of our type but in which total extinction was forbidden. This quantity also displayed a fast decaying tail.

In the case of Lévy bugs the tail of $\rho(x)$ follows instead a power law, $\rho(x) \sim x^{-(2+\mu)}$, see Fig. 4b, arising from the long jumps. Note that, in the present case of circular symmetry, the relation $\rho(x, y)dx dy = R(r)(2\pi)^{-1}dr d\theta$ of $\rho(x, y)$ with the radial density of the average cluster, $R(r)$, where r and θ are the polar coordinates centered at the cluster center, implies $\rho(x) = R(r = |x|)(2\pi|x|)^{-1}$, so that the asymptotic behavior of the radial density is $R(r) \sim r^{-(1+\mu)}$. This is the same asymptotic behavior as the individual radial jumps in (8) and it is also the asymptotic tail of the probability of displacement from the original position of nonreproducing bugs moving by Lévy flights [19]. We note also that, for $\kappa = \kappa_\mu$, the central part of $\rho(x)$ is narrower and higher in the Lévy than in the Brownian bug system, and it is narrower and higher the smaller the value of μ (see Fig. 4a). This is a somehow counterintuitive effect of the Lévy motion on clusters, already commented in the noninteracting case: increasing anomalous diffusion (smaller μ) induces larger jumps and longer tails, but at small scales it acts as making the cluster more compact.

The influence of the diffusivity is similar in both systems: the larger is the value of κ or κ_μ the more spread is the average cluster (see Fig. 5). For the Brownian one-dimensional case it was shown in Ref. [7] that cluster width is essentially the distance associated to the Brownian walk during the lifetime of a bug and their descendants. Thus, the width increases as $\kappa^{1/2}$. In the Lévy case, defining the distance associated to the walk is more subtle, since higher moments of displacements diverge. But the behavior of lower ones and dimensional analysis indicate that typical displacements during a lifetime scale as $\kappa_\mu^{1/\mu}$, and then this should determine the width of $\rho(x)$ or $R(r)$ (i.e., the spatial dependence should occur only through the combinations $[x\kappa_\mu^{-1/\mu}]$ or $[r\kappa_\mu^{-1/\mu}]$). Imposing additionally that the total number of bugs in the average cluster in this global interaction case does not depend on particle motion or distribution, and it is thus independent on the value of κ_μ we have $R(r) = \kappa_\mu^{-1/\mu} F(r\kappa_\mu^{-1/\mu})$, or

$$\rho(x) = \frac{1}{\kappa_\mu^{2/\mu}} G\left(\frac{x}{\kappa_\mu^{1/\mu}}\right), \quad (21)$$

with $G(u) = F(u)/u$. The analogous scaling form for the average cluster in the Gaussian diffusion case is

$$\rho(x) = \frac{1}{\kappa} G\left(\frac{x}{\kappa^{1/2}}\right). \quad (22)$$

The insets in Fig. 5 show the validity of these scaling forms.

In addition to the average cluster shape, which gives information on the cluster width, it is also interesting to study the fluctuations of the cluster width in time. We characterize cluster width at each instant of time by the standard deviation of the bug positions with respect to the center of mass of the cluster at that time. Then, a probability density $\pi(\sigma)$ is constructed from the values

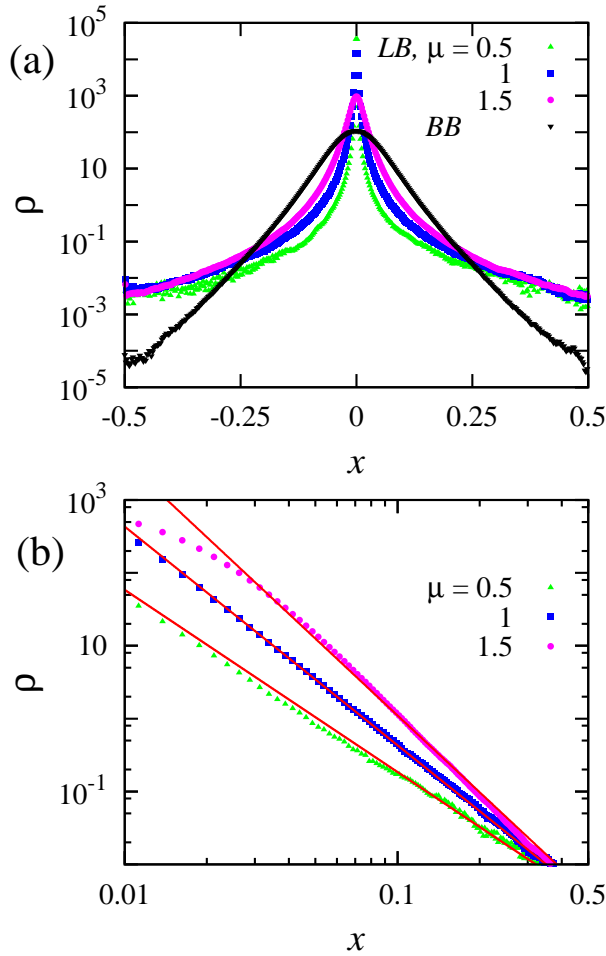


FIG. 4: (Color online) (a) $\rho(x)$, the cross-section of the two-dimensional particle density of the average cluster in semi-log scale; comparison between the Brownian and Lévy bug systems; $\kappa = 10^{-5}$, $\kappa_\mu = 10^{-5}$, $r_{b0} = 1$, $r_{d0} = 0.1$, $\alpha = 0.02$, $\beta = 0$. (b) The tails of $\rho(x)$ in log-log scale in the case of the Lévy bug systems for different values of μ . Solid lines correspond to fitting curves $\propto x^{-(2+\mu)}$.

of σ at different times. Figure 6 shows that in the case of globally interacting Brownian bugs the distribution of σ is short-tailed. In the case of globally interacting Lévy bugs, in contrast, the distribution for σ is characterized by tails with a power law decay with exponent $-(1+\mu)$. This means that in the latter case the cluster width can undergo arbitrarily large fluctuations in time. We note that the tails in $\pi(\sigma)$ decay with the same exponent as the radial density $R(r)$ of the average cluster, thus suggesting that the tails of the average cluster are produced by the large fluctuations in the width of the instantaneous clusters (which in fact include splitting events).

The individual motion of bugs drives the behavior of the center of mass of the system. Figure 7 depicts the probability density $p(\Delta_{CM})$ of the jump lengths Δ_{CM} performed by the center of mass each time the bug motion step is executed in the globally interacting Brownian and Lévy bug systems. For Brownian bugs it is short-

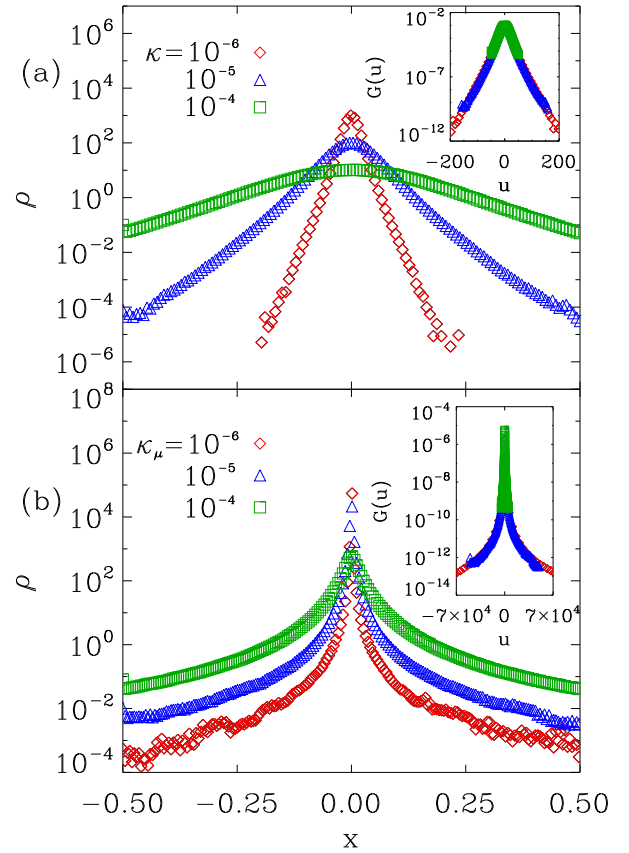


FIG. 5: (Color online) $\rho(x)$, the cross-section of the two-dimensional particle density of the average cluster in semi-log scale for different values of diffusivity: (a) Brownian bugs and (b) Lévy bugs with $\mu = 1$. Other parameters are as in Figs. 2 and 4. The insets check the correctness of the scaling forms (22) (with $G(u) = \kappa\rho$ and $u = x/\kappa^{1/2}$) and (21) (with $G(u) = \kappa_\mu^{2/\mu}\rho$ and $u = x/\kappa^{1/\mu}$).

tailed. In fact, from the arguments in Ref. [7], the center of mass motion of the cluster for globally interacting Brownian bugs is characterized by a Brownian process with the same diffusion coefficient as the individual bugs. In the case of Lévy bugs the probability density of the jump lengths of the center of mass is described by a distribution with a power-law tail with exponent $-(1+\mu)$, i.e., the center of mass of the cluster formed in the case of globally interacting Lévy bugs undergoes jumps that follow asymptotically the same law as the single bugs, Eq. (8), and as the radial tails of the average cluster. This reflects the fact commented previously that, due to the long jumps of the Lévy bugs, additional clusters far from the main one appear from time to time, strongly displacing the center of mass of the system. Due to the fluctuations it is even possible that the cluster that used to be the main cluster disappears and a new main cluster forms somewhere else. As a result the center of mass motion undergoes the same type of superdiffusion as the individual bugs of the system.

Extending the arguments for the Brownian bugs [7]

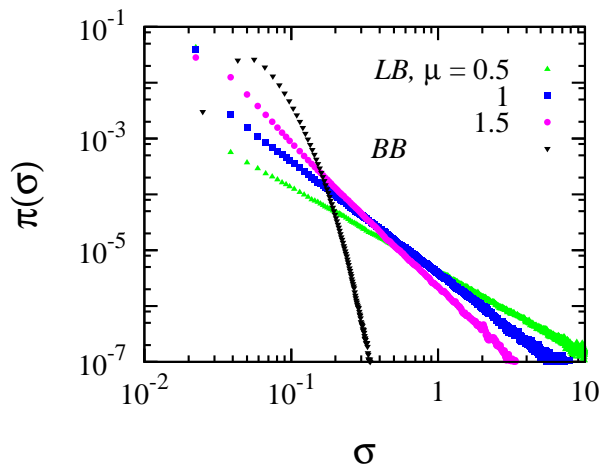


FIG. 6: (Color online) Probability density $\pi(\sigma)$ of the standard deviation σ of the bug positions with respect to the center of mass of the cluster in the Brownian and Lévy bug systems; $\kappa = 10^{-5}$, $\kappa_\mu = 10^{-5}$. The distribution is obtained averaging over a long time. The curves corresponding to the Lévy bug systems are well fitted by $\propto \sigma^{-(1+\mu)}$ (not shown). Other parameters are as in Figs. 2, 4, and 5.

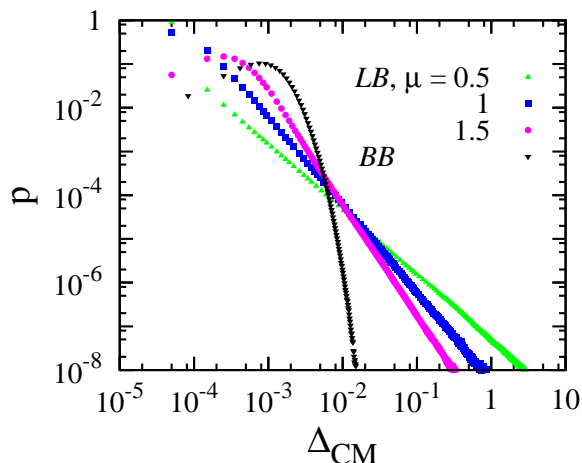


FIG. 7: (Color online) Probability density $p(\Delta_{CM})$ of the jump lengths of the center of mass in the Brownian and Lévy bug systems. Same parameter values as in Fig. 6. The tails of the curves corresponding to Lévy bugs are well fitted by $\propto \Delta_{CM}^{-(1+\mu)}$ (not shown).

(which were themselves adapted from the ones in [1]) to the Lévy case one can heuristically show that the distributions of σ and Δ_{CM} are related. To this aim one makes the approximation that the number of bugs in the system is constant, say N , instead of being constant on average. The center of mass receives a positive contribution from the new bugs appearing (at location \vec{x}_i) due to the reproduction between diffusion steps (say at time t_i), a negative contribution from the bugs disappearing during that time (say from position \vec{x}_j at time t_j), and the

direct contribution from the Lévy jumps $\vec{\ell}_k$ of all bugs present at the diffusion step:

$$\vec{\Delta}_{CM} = \frac{1}{N} \sum_{i \in B} \vec{x}_i(t_i) - \frac{1}{N} \sum_{j \in D} \vec{x}_j(t_j) + \frac{1}{N} \sum_{k=1}^N \vec{\ell}_k. \quad (23)$$

B and D denote the sets of bugs that have been born or dead, respectively, between diffusion steps. The two first terms can be combined in a single one $\vec{S} \approx N^{-1} \sum_{p=1}^n \vec{\sigma}_p$ by considering that the two sets have approximately the same number of individuals, n . $\vec{\sigma}_p = \vec{x}_i - \vec{x}_j$ is the displacement between a pair of these bugs, one just born and the other just disappeared, sampled inside the same cluster. Then the modulus of each σ_p should be of the order of the cluster width σ , which fluctuates in time with probability tails ruled by an exponent $-(1+\mu)$. This contribution in Eq. (23) gives the motion of the center of mass due to the birth and death processes. The contribution from the individual particle jumps is in the last term in (23), which is a sum of Lévy jumps of parameter μ so that the tails of the probability density are characterized by a decay with the same exponent $-(1+\mu)$. These heuristic arguments imply that the modulus Δ_{CM} will also be distributed with long tails characterized by an exponent $-(1+\mu)$, as observed.

V. NONLOCAL INTERACTION

A. Formation of a periodic pattern

In Refs. [6, 8, 9] on the nonlocally interacting Brownian and Lévy bugs it was assumed that the birth and death rates of the i -th individual are given by Eqs. (14), (15). In the case of Brownian bugs, for small enough diffusion coefficient and large enough Δ_0 , the occurrence of a periodic pattern consisting of clusters that are arranged in a hexagonal lattice was observed (see Fig. 8a-c) [6, 8]. For large values of the diffusion coefficient such periodic pattern is replaced by a more homogeneous distribution of bugs (Fig. 8d). In the case of Lévy bugs, since the diffusion coefficient (6) is infinite, one could expect that the spatial distribution will not reveal a periodic pattern; however, as shown in Ref. [9], for proper parameters periodic cluster arrangements do indeed occur (see Fig. 9). The reason for the divergence of the diffusion coefficient in the Lévy case is in the statistical weight of large jumps. These large jumps have some influence on the characteristics of the pattern formed, but the relevant structure is ruled mainly by the interactions between individuals. In the Lévy bug system however, at variance with the Brownian case, even at small values of κ_μ there are many solitary bugs appearing for short time periods in the space between the periodically arranged clusters due to the large jumps [9], c.f. Figs. 8a and 9a. However, the periodicity of the pattern is of the order of R (the interaction range) in both systems, being only

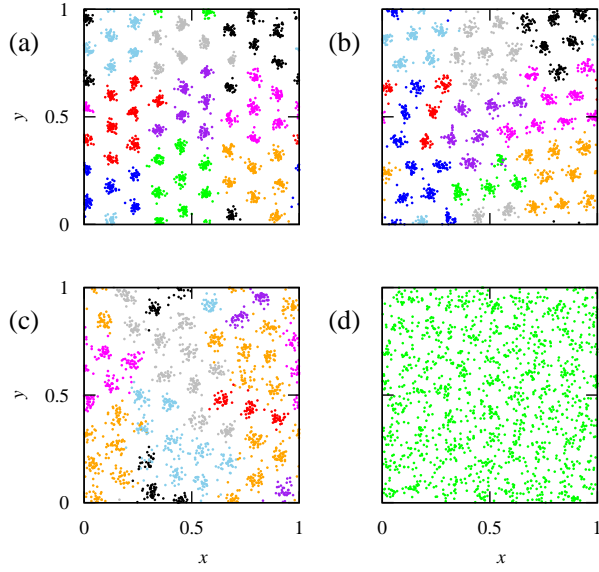


FIG. 8: (Color) Interacting Brownian bug model with $R = 0.1$, $r_{b0} = 1$, $r_{d0} = 0.1$ and $\alpha = 0.02$, $\beta = 0$. Spatial configuration of bugs at time 45000 in systems with different diffusion coefficients: (a) $\kappa = 10^{-5}$, (b) $\kappa = 2 \times 10^{-5}$, (c) $\kappa = 4 \times 10^{-5}$, (d) $\kappa = 10^{-4}$. The initial configuration of bugs is the same as in Figs. 1 and 2 at time $t = 0$.

slightly influenced by κ or κ_μ and μ , as demonstrated in Refs. [6, 9] through a mean-field theory calculation.

In Ref. [9] also the two-dimensional particle density of the average cluster, obtained by setting the origin at the center of mass of each cluster forming the periodic pattern and averaging over all the clusters in the simulation area and over time, was studied. In both, Brownian and Lévy bug systems the central part of the average cluster, where most of the individuals are concentrated, was well fitted by a Gaussian function, but the way the particle density decreases when moving away from the center of mass of the cluster is rather different. In the Brownian case a Gaussian decay provides a good approximation, whereas in the Lévy case it is close to exponential. The comparison with the systems with global interaction, discussed in Sec. IV C, reveals therefore that the interaction range R turns the exponential decay into Gaussian and the power law decay into exponential.

For a given value of diffusion coefficient, there exists a critical value of Δ_0 below which the system gets extinct, independently of α [6]. Above this critical value, for every α the increase of Δ_0 results in the increase of the average number of bugs, but the pattern formation is not much influenced. The latter is, however, true solely if Δ_0 increases through the increase of r_{b0} and the death rate is low. Namely, as in the case of global interaction discussed in Sec. IV B, an increase of the death rate, though accompanied by a compensating increase of birth rate, leads to larger fluctuations in the particle number. In numerical simulations we have observed that the larger are the fluctuations in the number of bugs, the more dif-

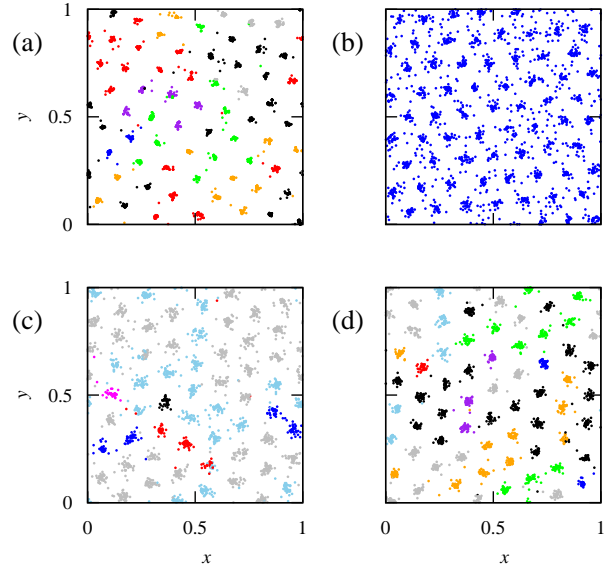


FIG. 9: (Color) Interacting Lévy bug model with $R = 0.1$, $r_{b0} = 1$, $r_{d0} = 0.1$ and $\alpha = 0.02$, $\beta = 0$ (same parameters as in Fig. 8 for Brownian bugs). The spatial configuration of bugs at time 45000 in systems with different generalized diffusion coefficients and anomalous exponent: (a) $\kappa_\mu = 10^{-4}$, $\mu = 1$; (b) $\kappa_\mu = 10^{-3}$, $\mu = 1$; (c) $\kappa_\mu = 10^{-4}$, $\mu = 1.5$; (d) $\kappa_\mu = 5 \times 10^{-5}$, $\mu = 1.5$. The initial configuration of bugs is the same as in Figs. 1 and 2 at time $t = 0$.

ficult is the formation of the periodic pattern, and finally the individuals do not arrange in the periodic pattern but in random clusters (see also Ref. [16]). This effect may in fact make difficult to observe the periodic clustering phenomenon in real competitive biological systems.

In the following we keep for the parameters in the birth and death rate the same values as in the case of global interaction, i.e., $r_{b0} = 1$, $r_{d0} = 0.1$, $\alpha = 0.02$, $\beta = 0$. For these parameter values the number of bugs fluctuates only weakly around the mean value. Differently from the case of global interaction, now the average number of bugs in the system is influenced not only by the birth and death rates, but also by the diffusion, i.e., in the case of Brownian bugs by κ and in the case of Lévy bugs by κ_μ and μ , see Fig. 10. The smaller is κ , κ_μ or μ , the larger the particle number. At the same time Figs. 8 and 9 indicate that by decreasing κ or κ_μ the linear width of the clusters becomes smaller, the particle density in the clusters higher, and the density between the clusters lower (c.f. Sec. IV C and see also Ref. [9]). Somehow counter-intuitively, the effect of decreasing μ seems to have the same effects, as commented above for the noninteracting and global cases. Furthermore, the value of κ or κ_μ and μ seems to weakly influence the number of clusters in the system: In Figs. 8 and 9 smaller values lead to larger number of clusters. This observation is not explained by the linear instability analysis of [6, 9].

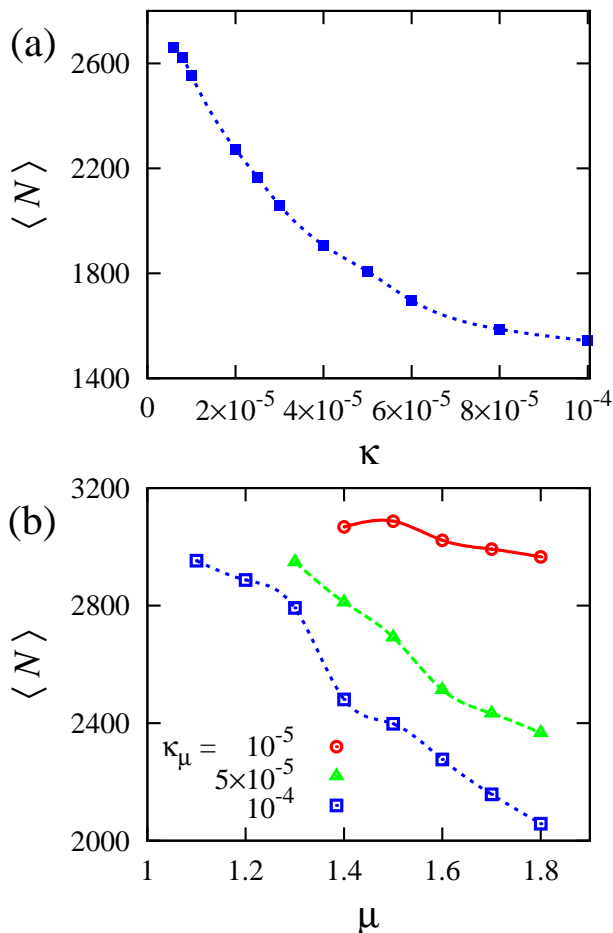


FIG. 10: (Color online) a): Average number of bugs versus diffusion coefficient in the system with Gaussian jumps. b): Average number of bugs versus anomalous exponent μ in the system with Lévy jumps for various values of the anomalous diffusion coefficient. Other parameters as in Figs. 8 and 9.

B. Mixing of different families

It is interesting to study the evolution of the system also regarding the disappearance or survival of the different groups, by dividing initially the bugs into different families and following their descent. In the case of nonlocally interacting Brownian bugs, a very low diffusion coefficient leads to the situation in which after cluster formation the inter-cluster travel is very rare because the individuals are not capable to make the jumps from one cluster to another one, and it is also very unlikely to arrive to the next cluster doing a multistep random walk because death is very probable between the clusters. Therefore, in the case of very low diffusion different families would remain inside their initial clusters. If one assumes that initially each individual represents a different family, then only inter-cluster competition occurs and the final number of families is equal to the number of clusters. If instead initially individuals are assigned

to families according to large areas of initial positions (larger than typical cluster size as done in Figs. 1 and 2 at time $t = 0$), there is no family competition internal to the clusters, most families survive and the clusters coming from different families occupy approximately the territory of the ancestors even after a long time, as can be seen from Fig. 8a. In that case, the travel of a cluster to a new territory away from the other clusters of the same family can take place due to the diffusion of the cluster as a whole during the clusters arrangement into the periodic pattern. For larger values of κ the inter-cluster travel is possible which leads to the conquering of new territories, i.e., bugs can be found in a region where their ancestors were not from, Fig. 8b. The effect is larger for larger κ and leads to the disappearance of some families, as can be seen from Fig. 8c. Finally, for increased diffusion, intra-cluster competition will force all surviving bugs to be from a single family (in fact, from a single ancestor); which family (ancestor) wins is a random event. The process is faster for larger diffusion. Increasing the diffusivity further even the periodic pattern disappears, Fig. 8d.

Figure 9 illustrates the family mixing for nonlocally interacting Lévy bugs. In this case the inter-cluster traveling is supported by the long jumps. Differently from the case of Brownian bugs, now the individuals can reach not only the next neighboring cluster but also clusters far away. Consequently, a cluster originally consisting of bugs coming from one ancestor can after some time turn into a cluster consisting of bugs coming from different families placed initially far away. Thus, intra-cluster bug competition becomes soon competition between families, and even if the diffusivity of the bugs is very low, at the end the Lévy bug system would consist of individuals coming from one or just a few ancestors. As in the case of Brownian bugs, the process of the disappearance of families is faster the greater is the generalized diffusion coefficient.

Besides the diffusion of a cluster as a whole during the formation of the periodic pattern and the conquering of new territories through the migration to and survival in another cluster, the mixing of clusters from different families can take place also due to the appearance of a new cluster if in the periodic pattern there is a dislocation. In the case of Brownian bugs the new cluster is formed through the splitting of an old cluster. In the case of Lévy bugs, instead, the new cluster can appear also far from the original territory.

VI. CONCLUSIONS AND OUTLOOK

We have presented some detailed properties of interacting particle systems in which the individuals are Brownian or Lévy random walkers which interact in a competitive manner. We have seen strong differences between the globally and the finite-range nonlocally interacting systems. In the systems with global interaction the spa-

tial distribution of the bugs becomes tied to the type of diffusion, Brownian or Lévy. Typical configurations consist of a single or a few clusters for both types of motion. For the Lévy bug systems long tails appear in the mean cluster shape and in probability distributions of cluster width and of jumps of the center of mass. For Brownian bug systems these quantities appear to be much shorter ranged. This is qualitatively also the situation in the non-interacting case, although then the effects of the particle-number fluctuations are much stronger. Under non-local finite-range interactions the situation is rather different. First, single cluster configurations are generally replaced by periodic patterns with periodicity set by the interaction range R . Motion of individual clusters is severely restricted by the presence of the neighboring clusters. In addition, the natural spatial cut-off introduced by the interaction range R seems to limit the influence of the long Lévy jumps, so that measures of spatial cluster shape do not generally exhibit power laws, making spatial configurations under both types of diffusion more similar. Mixing of families and their competition is nevertheless greatly influenced by the type of motion. This suggests that it would be interesting to consider the influence of different types of diffusion into competitive genetic mixing processes [22].

Obtaining analytic understanding in this type of interacting systems is difficult, but at least the nature of the instability leading to pattern formation and its relevant spatial scale have been clarified by using partial integro-differential equation descriptions of the mean field type [6, 9], which are useful in broader contexts [23–25]. However, from previous work in the Gaussian case [7, 8, 26], it is known that quantities such as cluster width and structure or transition thresholds strongly depend on particle-number fluctuations. Thus, obtaining additional results from differential equation approaches would need the inclusion of effective multiplicative noise terms [5] or focus on statistical quantities such as pair correlation functions [2, 16, 27].

Acknowledgments

This work has been supported by the targeted financing project SF0690030s09, Estonian Science Foundation through grant no. 7466, by the Balearic Government (E.H.), and by Spanish MICINN and FEDER through project FISICOS (FIS2007-60327).

-
- [1] Y.-C. Zhang, M. Serva, and M. Polikarpov, *J. Stat. Phys.* **58**, 849 (1990).
 - [2] W. R. Young, A. J. Roberts, and G. Stuhne, *Nature* **412**, 328 (2001).
 - [3] J. Felsenstein, *The American Naturalist* **109**, 359 (1975).
 - [4] B. Houchmandzadeh, *Phys. Rev. Lett.* **101**, 078103 (2008).
 - [5] F. Ramos, C. López, E. Hernández-García, and M. A. Muñoz, *Phys. Rev. E* **77**, 021102 (2008).
 - [6] E. Hernández-García and C. López, *Phys. Rev. E* **70**, 016216 (2004).
 - [7] E. Hernández-García and C. López, *J. Phys.: Condens. Matter* **17**, S4263 (2005).
 - [8] C. López and E. Hernández-García, *Physica D* **199**, 223 (2004).
 - [9] E. Heinsalu, E. Hernández-García, and C. López, *Europhys. Lett.* **92**, 40011 (2010), Erratum: **95**, 69902 (2011).
 - [10] P. Dieterich, R. Klages, R. Preuss, and A. Schwab, *Proc. Natl. Acad. Sci. USA* **105**, 459 (2008).
 - [11] D. Sims, E. Southall, N. Humphries, G. Hays, C. Bradshaw, J. Pitchford, A. James, M. Ahmed, A. Brierley, M. Hindell, et al., *Nature* **451**, 1098 (2008).
 - [12] F. Bartumeus, M. G. E. D. Luz, G. M. Viswanathan, and J. Catalán, *Ecology* **86**, 3078 (2005).
 - [13] M. Levandowsky, B. S. White, and F. L. Schuster, *Acta Protozool.* **36**, 237 (1997).
 - [14] M. de Jager, F. J. Weissing, P. Herman, B. A. Nolet, and J. van de Koppel, *Science* **332**, 1551 (2011).
 - [15] E. Brigatti, V. Schwammle, and M. A. Neto, *Phys. Rev. E* **77**, 021914 (2008).
 - [16] D. A. Birch and W. R. Young, *Theoretical Population Biology* **70**, 26 (2006).
 - [17] W. H. Press, B. P. Flannery, S. A. Teulolsky, and W. Vetterling, *Numerical Recipes in C: The Art of Scientific Computing* (Cambridge University Press, Cambridge, 2 edition, 1992).
 - [18] R. Klages, G. Radons, and I. M. Sokolov, *Anomalous Transport: Foundations and Applications* (Wiley-VCH, 2008).
 - [19] R. Metzler and J. Klafter, *Phys. Rep.* **339**, 1 (2000).
 - [20] J. P. Nolan, *Stable Distributions - Models for Heavy Tailed Data* (Birkhauser, Boston, 2012), to appear. Chapter 1 online at <http://academic2.american.edu/~jpnolan>.
 - [21] C. R. Doering, K. V. Sargsyan, and L. M. Sander, *Multiscale Modeling & Simulation* **3**, 283 (2005).
 - [22] H. Sayama, M. A. M. de Aguiar, Y. Bar-Yam, and M. Baranger, *Phys. Rev. E* **65**, 051919 (2002).
 - [23] M. A. Fuentes, M. N. Kuperman, and V. M. Kenkre, *Phys. Rev. Lett.* **91**, 158104 (2003).
 - [24] M. G. Clerc, D. Escaff, and V. M. Kenkre, *Phys. Rev. E* **72**, 056217 (2005).
 - [25] Y. E. Maruvka and N. M. Shnerb, *Phys. Rev. E* **73**, 011903 (2006).
 - [26] E. Hernández-García and C. López, *Physica A* **356**, 95 (2005).
 - [27] B. Houchmandzadeh, *Phys. Rev. E* **80**, 051920 (2009).